

# MORPHING STRUCTURES TECHNOLOGY AND ITS APPLICATION TO FLIGHT CONTROL

Thomas K. Bliss and Dr. Hilary Bart-Smith

Department of Mechanical and Aerospace Engineering, University of Virginia, Charlottesville, Virginia

## Abstract

The common goal of all aerospace advancements is safe, efficient air transportation. Current methods for achieving directional stability—control surfaces such as flaps and ailerons—are heavy and inefficient. If these bulky mechanisms were replaced with an ultra-lightweight morphing structure, efficiency could be increased by cutting drag and weight. In this project, an active truss structure has been designed and tested to examine its load carrying and morphing capabilities. Actuators replace passive members in this structure to achieve shape change. Project goals include modeling, constructing, and deflection analysis of a morphing system. The system is built using a rapid prototype-milling machine at the University of Virginia. An analytical solution to describe the deflection of the structure has been derived and compared with experimental results. Initial results have demonstrated the potential of these structures for use as a control surface.

## I. Introduction

This project is a proof of concept design to illustrate the use of morphing structures as an efficient means of flight control. A morphing structure has been constructed using a truss and actuator system. It is envisioned that this structure could form part of the trailing edge of a wing. This internal flap system is optimized for strength and output force. The system demonstrates that morphing structures have the ability to control airflow, as well as to increase efficiency through weight savings over current technologies.

In a crude aircraft constructed of wood and muslin, Orville Wright took to the skies for a seemingly endless twelve seconds. Those twelve seconds heralded a new era of technological ability. They would push the frontiers that man could not envision overcoming only a few years prior to this breakthrough. In just 35 years since the Wright brothers' historic flight, aeronautics took us from the blistering winds of Kill Devil Hills to the "high untrespassed sanctity of space" Pilot Officer Magee reached in his Spitfire.<sup>1</sup> Magee's freedom of flight – "touching the face of God" – became accessible to generations<sup>1</sup>. Humans, by nature, will always reach to the heavens, and the field of aeronautics propels them.

Many wing designs have carried man into the blue, some fast, some slow, but all based on the fluid mechanics of lift and drag. The Wright brothers relied on wing warping to control the roll and yaw of their flier, but as the airplane became more advanced, stronger wing structures were required to lift the fuselage off the ground. Muslin and flexible ash did not have the stiffness and strength requirements for such structures. The next generations of airfoils were manufactured from much stiffer materials, such as aluminum, but with this it became necessary to design the wings with movable flaps and ailerons for flight control. These additions result in a significant weight

increase and reduce the overall efficiency of the system by increasing drag. I hope to study the possibility of replacing these systems with an ultra lightweight structure that can change shape when necessary to control flow and reduce drag, thereby increasing fuel efficiency.

The objectives of this project are to design a two-dimensional statically determinate truss structure, which contains linear actuators as replacement for some of the passive truss members, and to test and analyze the actuation response of this structure in the presence of an applied load. Based upon previous work (Lu *et al.*<sup>2</sup>) a structural foundation is designed and fitted with linear actuators. Data will be collected analyzed to draw conclusions on the application of morphing structures to flight control.

This project has been divided into three phases: preliminary design, secondary design, and optimization and testing. For the primary design phase, a chemical wood model was produced. The next design stage was constructed from Delrin, a hard plastic. The final stage consisted of optimization of the structure and actuation system as well as testing of the system. These three phases will be discussed in detail in the following sections: Background, Methods and Materials, Deflection Analysis, Results, Discussion, and Conclusions.

## II. Background

Researchers have proposed an airfoil structure that can change shape on the fly, achieving the same aerodynamic affect as a flap, but at much less weight. Additionally, it has been shown that by continually monitoring the flight conditions, such a structure can morph the airfoil to the most efficient profile, significantly improving efficiency. Less flow around the wing would be blocked and the wing's wake would

be smaller, reducing drag. By incorporating strong, light truss structures inside the airfoil, weight will be reduced without sacrificing strength. In principle, this is a return to the Wright's method of wing warping. In a computer simulation, Gern *et al.* have shown that the rolling moment of a morphing wing compares to and outperforms conventional wing designs with flaps. They state two main reasons for the superior performance. First, the conventional wing exhibits a strong suction force at the flap hinge, reducing roll performance. Second, the morphing airfoil model is structurally stronger than that of the conventional wing.<sup>3</sup>

The principle behind the analysis of morphing structures is based upon Maxwell's necessary condition for statically and kinematically determinate structures.<sup>4,5,6</sup> By replacing passive members with actuators, significant shape changes can be attained. Lu *et al.* have shown that sandwiching a truss system between two shape memory alloys (SMA) can achieve large deflections (Figure 1). They have also noted that the truss structure has a relatively high strength-to-weight ratio. Lu *et al.* have developed a method to analyze the achievable displacement of a morphing structure under a load. This analysis will be adapted for application to this project. Their research has also provided a means to determine failure criteria and optimization of the truss structure.<sup>2</sup>

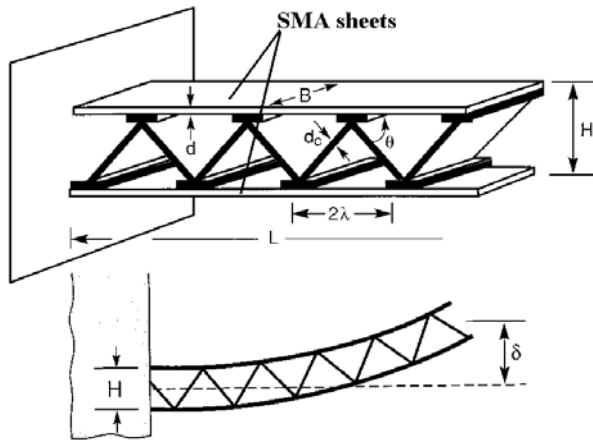


Figure 1 Statically determinate truss with actuation of top SMA sheet<sup>2</sup>

Risseeuw attempted to adapt morphing structures and SMA technology to a wing structure. He lined the inner side of the upper skin of an airfoil section with triangular trusses. NanoMuscles, small linear actuating SMAs, connected the truss points (Figure 2). When the NanoMuscles received voltage, they contracted, pulling the truss points closer, morphing the airfoil. Risseeuw ran into many problems with his design. Constructed of layered ABS plastic,

microscopic cracks spread on the wing during actuation. Structural integrity was compromised and the wing's ability to morph after repeated cycles fell. NanoMuscles also overheated and stiffened when strained for extended periods.<sup>7</sup>

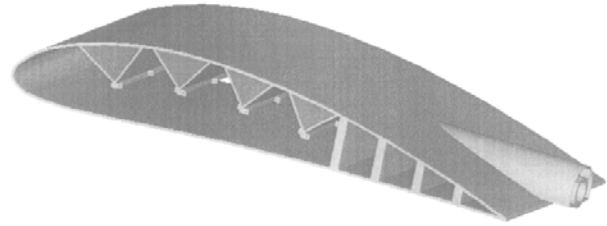


Figure 2 AutoCAD rendering of Risseeuw's morphing wing section<sup>7</sup>

With the correct materials and actuators, it is possible to build a successful morphing wing. The structure must be light, strong, and resistant to fatigue to avoid Risseeuw's results. Also, forceful actuators that can bear an extended load must be used. The resulting morphing wing "would be the mechanical equivalent of a bird that can shape change from eagle to hummingbird to hawk to seagull, on the fly, to better survive an environment in constant flux."<sup>8</sup>

### III. Methods and Materials

The goals of the project, as stated above, are to design, build, and test a high authority structure to illustrate the use of morphing structures as an efficient means of flight control. To do so, appropriate actuators, topological designs, materials, and construction techniques must be identified.

#### Actuator Selection and Optimization

Lu *et al.* and Risseeuw used SMAs or applied forms of SMAs to provide shape change in their morphing structures. With the negative results of Risseeuw's experiments, it is decided that these would not be the most effective actuators for this project. A more versatile and durable actuator is desired. Market research provided options such as solenoids, hydraulic actuators, and rotary servo motors. It was eventually decided to use linear stepper motors.

The chosen stepper motor is the z26000 series captive linear actuator. These are small actuators, one inch in diameter, produced by Haydon Switch & Instrument, Inc. (HSI). The z26443 has the highest achievable force output of the z26000 series and was therefore chosen for this project. The actuator is composed of a stepper motor, spinning around a non-rotating leadscrew that is fixed to the actuating shaft. This self-locking leadscrew design allows the actuator to hold any desired deflection without power

consumption. This is unlike SMAs which require a constant thermal input to maintain deflection.

Chopper Drive Cards, separate circuit boards purchased from HSI, control these linear actuators. These drive cards use an external DC power source between 24 and 40 Volts. The drive card contains a 555 timer to output pulses to the stepper motor in the actuator. By varying a potentiometer on the drive card, the step rate of the actuator can be varied, allowing one to control its speed and force output. As the step rate decreases, the force output increases as shown in Figure 3. A greater force output is desirable for the morphing structure concept; the speed of actuation is of lesser importance. Therefore, the drive cards are set up for a step rate of 100-125 pulses per second, realizing a force of approximately 60 Newtons. The drive cards also allow the actuators to be controlled externally by applying voltage inputs. LabView is used to provide these signals, controlling direction and actuation time.

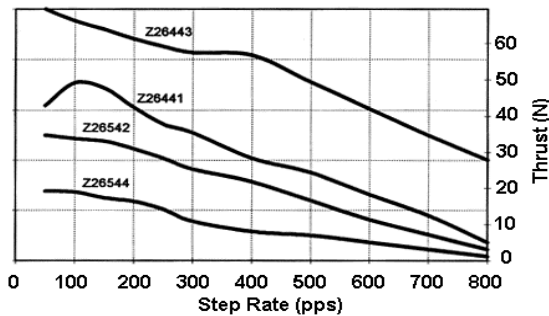


Figure 3 Output force as a function of step rate for the z26443 actuator<sup>9</sup>

### Topological Design

With actuator selection completed, the general structural design is to be determined. Based on Lu et al.'s work, the truss system will feature a triangular corrugation for three reasons. First, it will allow easy integration of the actuators. Second, "the triangulated configuration has exceptional bending stiffness that inhibits the counter deflection induced by the imposed forces and moments."<sup>2</sup> Third, "it offers no rotational resistance when comprised of frictionless-pinned joints."<sup>2</sup> This means that the actuators will not have to work against the structure when generating shape change. Lu et al. have also illustrated that this corrugation should feature base angles of 54.7° to maximize the transverse shear stiffness, and therefore withstand greater loads.<sup>2</sup>

### Preliminary Design

The goal of the first stage of the project is to determine if Haydon Switch & Instrument z26443 actuators can be effectively incorporated into a

morphing truss system. The working design created in this generalized stage will be carried over into all truss designs.

With the basic geometry determined above, the goal is to incorporate the z26443 actuator in the system. Risseeuw's design allowed for easy incorporation of NanoMuscles due to their small size and convenient pinning holes.<sup>7</sup> The z26443 actuators are more bulky and complex than NanoMuscles, and will therefore require a more complex mounting system. To avoid generating internal bending stresses in the trusses and actuators during actuation, all joints must be pinned and free to rotate. The structure designed as a result of these constraints is shown in the CAD rendering below (Figure 4). Key components that will be featured in the secondary design are the actuator yoke, shaft pin, retaining caps, and truss hinge mechanism.

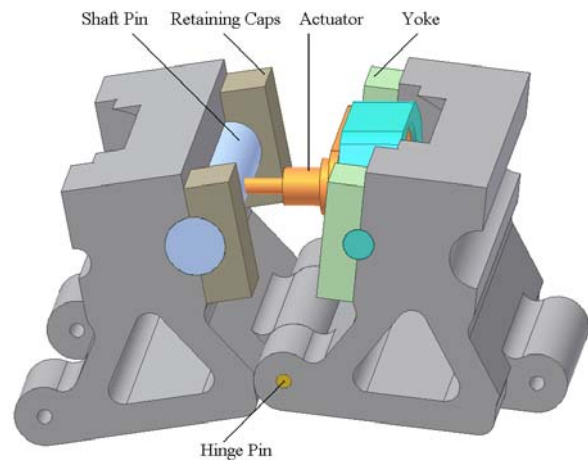


Figure 4 CAD rendering of Preliminary Design

All components are designed in Inventor7 and built on a Roland MDX-650 Prototype-Milling Machine using a 1/8" ball mill bit. Chemical wood is used for this stage of design because of its high machinability. The shaft pin is cut from 1/2" aluminum stock. Machine screws are used to attach the retaining caps to the truss bodies, and a 1/8" aluminum rod is used as the hinge pin between the two trusses. Figure 5 shows the successful assembly and actuation of the preliminary design. This structure is capable of deflections up to 17 mm.

### Secondary Design

With the successful construction of the preliminary design, a four-truss system is designed for both incorporation within an airfoil and deflection testing. A program called DesignFoil is used to determine what airfoil shape to be used in this design. DesignFoil features a full library of NACA four, five and six digit airfoils. Due to the large size of the

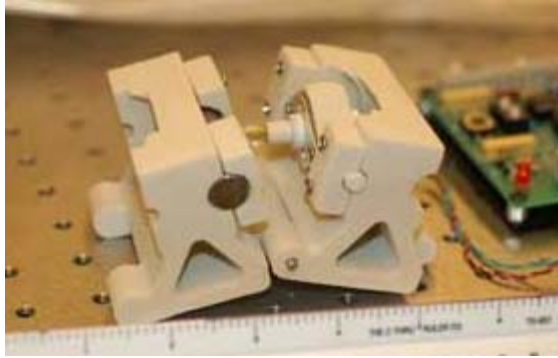


Figure 5 Image of completed preliminary design

z26443 actuators, the truss system designed will also be fairly large. This design constraint dictates that the airfoil chosen must be fairly thick to allow the truss system to fit inside. The chosen airfoil is the NACA 0018-63 because of its thickness and symmetry. A chord length of fifteen inches is chosen to allow for sufficient space inside the airfoil for the morphing structure. The structure designed as a result of these constraints is shown in the CAD rendering below (Figure 6).

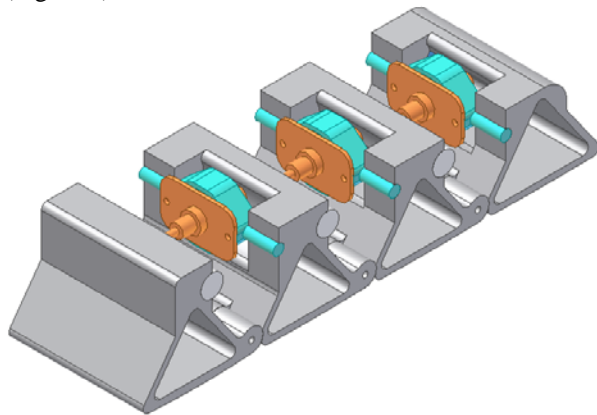


Figure 6 CAD rendering of secondary design

The secondary design is constructed using Delrin, a plastic with much greater strength and durability than chemical wood, yet is still easily machined. Due to its greater strength and density than chemical wood, a 1/4" mill bit is used on the MDX-650 to prevent damage and to speed up the cutting process. During final assembly of this truss system, the Mechanical Engineering Department's drill press and grinder are used to remove excess material from the trusses, yokes, and retaining caps. Again, the system includes rotational freedom at the yoke, shaft pin, and truss hinge (Figure 7). The four-truss system achieves astounding shape changes. Tip deflections up to 107.31 mm are possible, illustrating the effectiveness of this system. Although the truss system fits inside a wing structure in design, the actual morphing system

outperforms the airfoil structure. When fully morphed, the truss system no longer fits inside the airfoil.

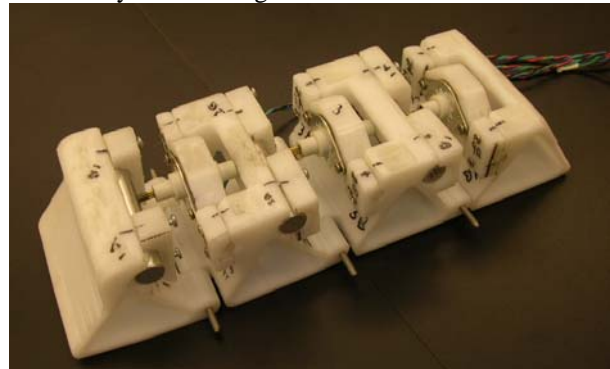


Figure 7 Image of completed secondary design

#### Test Rig Design

To test the deflection of the four-truss structure under actuation and loading, a test rig (Figure 8) is built to mount the four-truss system. This rig is two 2x4's notched to accept the first truss of the morphing structure. A threaded U-shaped retaining rod and back plate are used to fix the truss system to the rig. A T-square is clamped to the rig in parallel to the unactuated state of the structure to allow for consistent deflection measurements using digital calipers. The results from these experiments will be compared to the analytical model developed below.

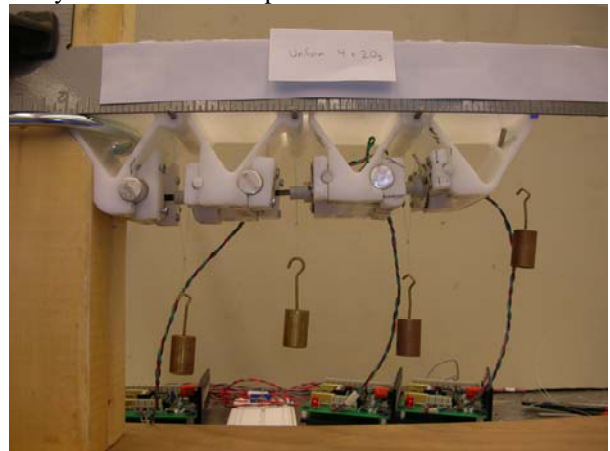


Figure 8 Image of deflection test rig

#### IV. Deflection Analysis

To illustrate the use of morphing structures as an efficient means of flight control, deflection test data will be compared to an analytical model. A loading and actuation deflection analysis adapted from Lu et al. will be developed to predict the capabilities of the structure.

### Static Analysis

The model illustrated in Figure 9 is used to approximate the structure created in the secondary

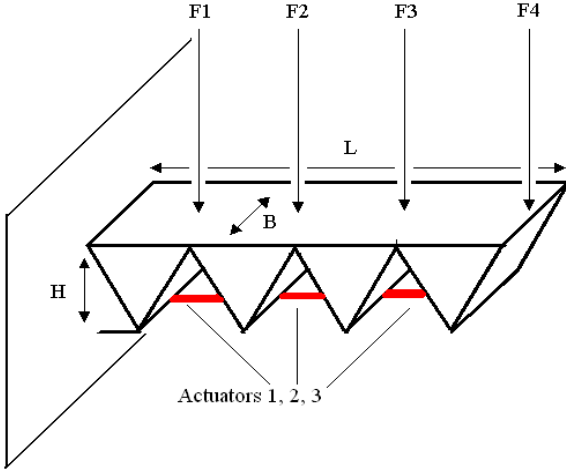


Figure 9 Geometry and configurations for analytical model

design. Although the analytical model is not exactly symmetric to the physical structure (Figure 7), the differences in geometry are assumed negligible, allowing a quicker, more powerful analysis of the truss system. Note that the aerodynamic pressures that the structure would experience have been simplified as point loads on the trusses. This static analysis results in the realization of the forces borne by each actuating member of the system as a function of external point loads and the geometry of the structure:

$$F_{A1} = -\frac{L}{4H}(F_2 + 2F_3 + 3F_4) \quad (1)$$

$$F_{A2} = -\frac{L}{4H}(F_3 + 2F_4) \quad (2)$$

$$F_{A3} = -\frac{L}{4H}F_4 \quad (3)$$

The analysis also resolves the forces and stresses within each non-actuating member of the system.

### Deflection Analysis

Next, using the method outlined by Lu et al., the end deflection of the truss system can be determined as a function of the actuation strains, the geometry of the structure, and the external loads applied.<sup>2</sup> Note that the method of superposition is used to analyze and combine the four separate loads on the truss. This method can be applied because the system is linear. The total deflection of the truss structure is a function of the deflection due to loading and deflection due to actuation,

$$\delta_0 = \delta_1 + \delta_{2,tot} \quad (4)$$

where the deflection due to actuation is,

$$\delta_1 = H \left( \frac{1}{2} + \frac{L}{\Delta L} \right) \left( 1 - \cos \left( \frac{\Delta L}{H} \right) \right) \quad (5)$$

and the total deflection due to loading is,

$$\delta_{2,tot} = \sum_{n=1}^4 \delta_{2,n} \quad (6)$$

The deflection due to  $F_n$  is

$$\delta_{2,n} = \left( \frac{F_n}{E_f B} \right) \left( \frac{2 \left( \frac{nL}{4} \right)^3}{3dH^2} + \frac{3\sqrt{3}nL}{4} \right) + \left( \left( 1 - \frac{n}{4}L \right) \left( \frac{\partial \delta_{2,n}}{\partial L} \right) \right) \quad (7)$$

where  $d$  is the wall thickness and

$$\frac{\partial \delta_{2,n}}{\partial L} = \left( \frac{F_n}{E_f B} \right) \left( \frac{2 \left( \frac{nL}{4} \right)^2}{dH^2} + \frac{3\sqrt{3}}{2d} \right) \quad (8)$$

The results of this analysis will be compared with the experimental deflections due to either actuation or externally applied load or a combination. This can be used to estimate the maximum load that can be applied to the structure, given the kinematic and material constraints.

## V. Results

### Deflection due to Actuation

To test the deflection due to actuation, the system is actuated to set strains with no loading, and the end tip deflection is observed. The data gained from this testing, shown in Table 1, are to be compared to  $\delta_l$ .

Table 1 Deflections due to actuation

|   | Actuator State (mm) |          | $\Delta L$<br>(mm) | Total $\Delta L$<br>(mm) | Deflection<br>(mm) |
|---|---------------------|----------|--------------------|--------------------------|--------------------|
|   | Home                | Actuated |                    |                          |                    |
| 1 | 8.3055              | 9.31     | 1.0045             |                          |                    |
| 2 | 13.181              | 14.455   | 1.274              |                          |                    |
| 3 | 8.73425             | 10.03275 | 1.2985             | 3.577                    | 12.985             |

|   | Actuator State (mm) |          | $\Delta L$<br>(mm) | Total $\Delta L$<br>(mm) | Deflection<br>(mm) |
|---|---------------------|----------|--------------------|--------------------------|--------------------|
|   | Home                | Actuated |                    |                          |                    |
| 1 | 8.183               | 10.143   | 1.96               |                          |                    |
| 2 | 13.19325            | 15.30025 | 2.107              |                          |                    |
| 3 | 8.70975             | 11.3925  | 2.68275            | 6.74975                  | 22.28275           |
| 1 | 8.2075              | 11.8825  | 3.675              |                          |                    |
| 2 | 13.09525            | 17.06425 | 3.969              |                          |                    |
| 3 | 8.624               | 12.397   | 3.773              | 11.417                   | 40.474             |
| 1 | 8.2075              | 13.90375 | 5.69625            |                          |                    |
| 2 | 13.21775            | 18.3015  | 5.08375            |                          |                    |
| 3 | 8.33                | 13.68325 | 5.35325            | 16.13325                 | 56.92575           |
| 1 | 8.232               | 15.52075 | 7.28875            |                          |                    |
| 2 | 13.181              | 19.649   | 6.468              |                          |                    |
| 3 | 8.61175             | 15.1165  | 6.50475            | 20.2615                  | 71.932             |
| 1 | 8.232               | 21.168   | 12.936             |                          |                    |
| 2 | 13.181              | 20.20025 | 7.01925            |                          |                    |
| 3 | 8.61175             | 17.70125 | 9.0895             | 29.04475                 | 107.4815           |

### Deflection due to Point Loads

The same test rig from actuation testing is used to measure the deflections due to loads. Weights are hung from the hinge pins using fishing line to simulate point loads. Weights ranging from 0 to 1 kg were tested on each of the four nodes for four trials. The deflections observed, to be compared to  $\delta_{2,tot}$ , are illustrated in Table 2. It is realized after these tests that the additional restraint is necessary to simulate the fixed boundary condition on the first truss. The data from this revised test step is shown in Table 3.

Table 2 Deflections due to point loading

| Mass (g) | Force (N) | Test 1 (mm) | Test 2 (mm) | Test 3 (mm) | Test 4 (mm) | Average (mm) |
|----------|-----------|-------------|-------------|-------------|-------------|--------------|
| 0        | 0         | 0           | 0           | 0           | 0           | 0            |
| 20       | 0.196     | 0.20825     | 0.20825     | 0.20825     | 0.20825     | 0.20825      |
| 50       | 0.49      | 0.637       | 0.47775     | 0.98        | 0.735       | 0.7074375    |
| 100      | 0.98      | 1.421       | 1.2005      | 1.47        | 1.45775     | 1.3873125    |
| 200      | 1.96      | 2.56025     | 2.695       | 2.78075     | 2.8665      | 2.725625     |
| 500      | 4.9       | 6.01475     | 6.35775     | 6.03925     | 6.01475     | 6.106625     |
| 1000     | 9.8       | 9.83675     | 9.849       | 9.9225      | 9.898       | 9.8765625    |

Table 3 Deflections due to point loading (revised test rig)

| Mass (g) | Force (N) | Test 1 (mm) | Test 2 (mm) | Test 3 (mm) | Average (mm) |
|----------|-----------|-------------|-------------|-------------|--------------|
| 100      | 0.98      | 0.53        | 0.47        | 0.57        | 0.523        |
| 200      | 1.96      | 0.93        | 0.97        | 1.03        | 0.977        |
| 500      | 4.9       | 2.29        | 2.35        | 2.45        | 2.363        |
| 600      | 5.88      | 2.66        | 2.76        | 2.67        | 2.697        |
| 700      | 6.86      | 3.05        | 3.2         | 3.12        | 3.123        |
| 750      | 7.35      | 3.4         | 3.44        | 3.33        | 3.390        |
| 1000     | 9.8       | 4.25        | 4.34        | 4.35        | 4.313        |

### Morphing Capabilities

The structure is tested to see under what loads it will no longer achieve shape change. It is expected that a load of 6.2 N (or a weight of 630 g) for each of the point loads will result in a resolved compressive force at the first actuator of 60 N. After loading the structure, actuation is attempted and it is found that the structure attains full range of motion up to an applied point load of 5.8 N (600 g).

## VI. Discussion

### Deflection due to actuation

The results from the deflection due to actuation prove to follow the model closely as can be seen in Figure 10. The data may not follow exactly due to the fact that the model approximated the actual geometry of the system. Other sources of error may include less than perfect tolerances of parts and assembly.

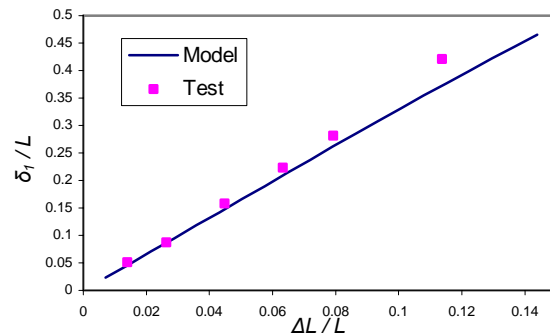
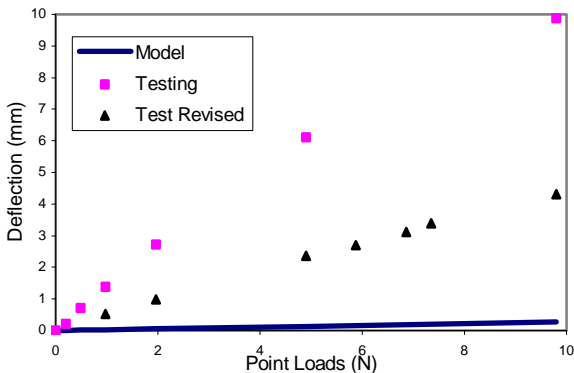


Figure 10 Graph of deflection due to actuation

### Deflection due to loading

The results from the load deflection testing are less promising (Figure 11). The analytical model illustrates the truss system as a stiff structure, allowing a tip deflection of only 0.13 mm under four point loads of 9.8 N each. When this loading scheme was tested on the secondary design structure, an average deflection of 9.9 mm was observed. With errors this large, the test rig was revised to include a hose clamp to add additional constraint to better simulate the fixed end boundary condition. Under the loading parameters mentioned above, the new average deflection was 4.3 mm. This illustrates that the primary source of error resides in test rig construction as well as truss construction. With so many components in the four-truss system, it is not surprising that machining and assembly imperfections could contribute to a large deflection error under loading. It is expected that as tolerances in construction increase in quality, the four-

truss system will better represent the analysis adapted from Lu *et al.*



Morphing capability testing provided positive results. It was expected that a point loadings of 6.2 N (630g) would result in compressive forces equal to the output force of the z26443 actuators. Weights were increased in small increments from 500g up to 630g and actuation of the system was attempted. The system failed at applied loads above 5.88 N (600g). Using the model illustrated in Figure 6, the maximum resolved compressive force on an actuator is 57.2 N. With the results fitting the hypothesis this closely, predictions of the morphing capabilities are considered successful.

## VII. Conclusions

All goals of the project were adequately met. A preliminary design was constructed and illustrated that the selected actuators could be effectively incorporated into a morphing truss system. The secondary design proved that large deflections could be achieved using four trusses and three actuators. The testing of this structure proved the accuracy of the static analysis as well as the accuracy of the deflection due to actuation. The testing of deflection due to loading illustrated room for improvement by using better construction techniques and materials. The testing of morphing capabilities also proves the accuracy of the static analysis and illustrates the large forces a morphing structure can handle.

This project illustrates the feasibility for morphing structures to be applied to flight controls. The morphing structure designed illustrates efficient, wide ranges of deflections under large loading parameters. The actuation system uses very little electrical power and is capable of holding any desired deflection without power consumption because of the self-locking pitch of the leadscrew. This is unlike SMA's, which require a current to generate heat while deflecting. The use of the linear stepper motors also

shows that off-the-shelf products are capable of the demands of morphing control systems.

Future research in the field of morphing structures for flight control should focus on adapting designs like the one created in the secondary design to trailing edges, leading edges, or the overall design of an airfoil. These structures should be tested for deflection as was carried out in this project. Tolerances and machining techniques should be improved over this design. It is also recommended that feasibility study be carried out to determine the output force requirements for actuators in a truss structure based on the aerodynamic forces experienced in flight.

## Acknowledgements

The authors would like to thank Louis Steva for his assistance in the manufacturing process. The authors would also like to thank the Harrison family for their support as well as VSGC for their funding of this work.

- <sup>1</sup> "High Flight." Pilot Officer John G. Magee, Jr. – US Air Force Museum Pre-WWII History. 28 April 2003 <[www.wpafb.af.mil/museum/history/prewwii/jgm.htm](http://www.wpafb.af.mil/museum/history/prewwii/jgm.htm)>.
- <sup>2</sup> Lu, T.J., Hutchinson, J.W., and Evans, A.G. "Optimal design of a flexural actuator." Journal of Mechanics of Solids and Structures 49 (2001): 2071-2093.
- <sup>3</sup> Gern, F.H., Inman, D.J., and Kapania, R.K. "Structural and Aeroelastic Modeling of General Planform Wings with Morphing Aerofoils." AIAA Journal 40.4 (2002): 628-637.
- <sup>4</sup> Maxwell, J.C. (1864). On the calculation of the equilibrium and stiffness of frames. Philosophical Magazine 27: 294-299.
- <sup>5</sup> Maxwell, J.C. (1890). Collected papers, XXVI. Cambridge University Press.
- <sup>6</sup> Deshpande, V.S., Ashby, M.F., and Fleck, N.A. "Foam Topology Bending Versus Stretching Dominated Architectures." Acta Mater 49 (2001): 1035-1040.
- <sup>7</sup> Risseuw, Phillip. "Airflow Control Through Morphing Structures." Fourth Year Thesis. University of Virginia. 2003.
- <sup>8</sup> ALLSTAR Network. "Conventional Aerofoils and Laminar Flow Aerofoils". Aeronautic Learning Library for Science, Technology, and Research. 12 March 2004 <<http://www.allstar.fiu.edu/aerojava/Wing31.htm>>.
- <sup>9</sup> Haydon Switch & Instrument. "Performance Curves". Linear Actuators – HSI Series z26000. 2003 <<http://www.hsomotors.com/linear-actuators/index.htm>>.